

FINAL REPORT

1 General Information

DFG reference number: WE4100/23-1

Project number: 387344394

Project title: **“Changing the wettability and barrier properties for bioplastics by plasma generated amorphous carbon coatings”**

Name of the applicant: Prof. Dr. Stefan Wehner

Official address: University of Koblenz, Universitätsstraße 1, 56070 Koblenz

Name(s) of the co-applicants: Dr. Christian B. Fischer (FI 1802, initially)

Name(s) of the cooperation partners: Prof. (UM6P) Dr. Christian B. Fischer (finally)

Reporting period (entire funding period): 01.05.2019 - 31.12.2024

2 Summary

Biodegradable polymers are promising alternatives to conventional petroleum-based materials, but their wider use is limited by poor surface properties, as improper wettability and unfavorable barrier properties. These disadvantages can be avoided by coatings with thin amorphous hydrogenated carbon (a-C:H) resp. diamond-like carbon (DLC) layers produced by mild plasma-assisted chemical vapor deposition (PECVD). Their chemical composition mainly includes sp^2 - and sp^3 -bound C, whereby their respective proportions are responsible for resulting surface properties. Varying this ratio a wide range of surface properties can be achieved. The sp^2/sp^3 ratio can be controlled by various plasma parameters e.g. the deposition time or angle. Here various biopolymers are coated at different times and geometries in respect to the plasma. Layer properties are examined for their sp^2 and sp^3 content using synchrotron assisted methods, and supplemented by measures of their wettability and barrier properties (CA, SFE, WVTR). Across all studies, the sp^2/sp^3 bonding ratio was a function of layer thickness, which is closely related to the deposition angle. Thin (up to ~ 30 nm) and more directly deposited (0° to 60°) layers were generally richer in sp^3 bonding, transitioning to sp^2 -dominance as the layers grow thicker, exceeding the interlayer threshold (for PLA ~40 nm, PHB ~20 nm, PBAT ~25–30 nm), and when deposited in more indirect angles (150° to 180°) even at higher thicknesses. Wettability measures for stable films showed a high dependency on the deposition angle and the substrate. PLA showed angle-sensitive CAs and surface energy variations resulting in a significant barrier improvement when coated more directly at 0° to 60° (up to 47% reduction). In contrast, PHB displayed already an increase in the permeability after the O_2 -plasma pretreatment and earlier interlayer formation. In summary this study demonstrates the feasibility of a-C:H coatings using scalable methods and validates the ability to control surface energy, barrier performance and morphology via geometrical changing parameters.

Zusammenfassung

Biologisch abbaubare Polymere sind vielversprechende Alternativen zu konventionellen erdölbasierten Materialien, aber ihre breitere Anwendung wird durch schlechte Oberflächeneigenschaften, wie unzureichender Benetzbarkeit und ungünstiger Barriereeigenschaften, eingeschränkt. Diese Nachteile können durch Beschichtungen mit dünnen amorphen hydrierten Kohlenstoff- (a-C:H) bzw. diamantähnlichen Kohlenstoffschichten (DLC) vermieden werden, die mittels milder plasmaunterstützter chemischer Gasphasenabscheidung (PECVD) hergestellt werden. Ihre chemische Zusammensetzung umfasst hauptsächlich sp^2 - und sp^3 -gebundenes C, wobei ihre jeweiligen Anteile für die resultierenden Oberflächeneigenschaften verantwortlich sind. Durch Variation dieses Verhältnisses kann eine Vielzahl von Oberflächenei-

genschaften erzielt werden. Das sp^2/sp^3 -Verhältnis kann durch verschiedene Plasmaparameter, z. B. die Abscheidungszeit oder den Abscheidungswinkel, gesteuert werden. Hier werden verschiedene Biopolymere zu unterschiedlichen Zeiten und in unterschiedlichen Geometrien in Bezug auf das Plasma beschichtet. Die Schichteigenschaften werden hinsichtlich ihres sp^2 - und sp^3 -Gehalts mit Hilfe von Synchrotron-unterstützten Methoden untersucht, ergänzt durch Messungen ihrer Benetzbarkeit und Barriereigenschaften (CA, SFE, WVTR). In allen Studien war das sp^2/sp^3 -Verhältnis eine Funktion der Schichtdicke, in direktem Zusammenhang mit dem Abscheidungswinkel. Dünne (bis zu ~ 30 nm) und direkt abgeschiedene (0° bis 60°) Schichten waren im Allgemeinen reichhaltiger an sp^3 -Bindungen, wobei mit zunehmender Dicke der Schichten ein Übergang zu sp^2 -Dominanz stattfand, ebenso beim Übergang zum Interlayer (für PLA ~ 40 nm, PHB ~ 20 nm, PBAT ~ 25 – 30 nm), und wenn sie in indirekteren Winkeln (150° bis 180°) abgeschieden wurden, selbst bei höheren Schichtdicken. Die Benetzbarkeitsmessungen für stabile Filme zeigten eine hohe Abhängigkeit vom Abscheidungswinkel und vom Substrat. PLA zeigte winkelabhängige CAs und Oberflächenenergieveränderungen, die zu einer signifikanten Verbesserung der Barriereigenschaften führten, wenn es bei 0° bis 60° beschichtet wurde (Reduzierung um bis zu 47 %). Im Gegensatz dazu zeigte PHB bereits nach der O_2 -Plasmavorbehandlung und einer früheren Interlayerbildung eine Erhöhung der Permeabilität. Zusammenfassend zeigt diese Studie die Darstellung von a-C:H-Beschichtungen unter Verwendung skalierbarer Methoden und bestätigt die Möglichkeit, die Oberflächenenergie, die Barriereigenschaften und die Morphologie durch geometrische Änderungsparameter zu steuern.

3 Progress Report

- Background

Shrinking raw material reserves and increasing volumes of especially plastic waste present a significant challenge for conventional polymers. However, polymers are frequently used in everyday life due to their advantageous properties and difficult to replace. Therefore, it is necessary to identify alternatives that are based on sustainable raw materials, are biodegradable, and still offer comparable properties. Like conventional polymers, biopolymers also have certain limitations. These include e.g. low hardness and high water vapor transmission rates (WVTR) which restrict their use for specific applications (food packaging, medical field).^[1,2] To change specific surface properties on polymers the deposition of amorphous hydrogenated carbon (a-C:H) resp. diamond-like carbon (DLC) layers using radio-frequency plasma-enhanced chemical vapor deposition (RF-PECVD) is an established technique.^[3-7] These layers consist of sp^2 - and sp^3 -bonded C-atoms along with hydrogen, which determine the surface properties depending on their relative ratio to each other. The sp^2/sp^3 ratio as well as the H-

content in these layers and consequently their chemical composition can be changed by varying plasma parameters.^[6,8-11] Therefore, a wide portfolio of surface properties can be achieved by adjusting the sp^2/sp^3 ratio, which allows the physical properties to be controlled. These carbon coatings pose a particular challenge for polymers, as the chemical and physical properties of the original surface change continuously or gradually during the coating process and an interlayer region of varying thickness is formed between both.^[12,13] Furthermore, a distinct interlayer is expected for a good connectivity between the layer and the polymer (= substrate effect). The thickness of the interlayer can be determined by means of synchrotron supported measures.^[14] In addition, the sp^2 to sp^3 ratio can be used to draw conclusions about the surface properties, compared with other methods (DRIFT, contact angle (CA), surface free energy (SFE), AFM, SEM) and complemented by measurements of the barrier properties for water. Within the project the surface of different biopolymers (polylactic acid – PLA; polyhydroxybutyrate-(valerate) PHB(V); polybutylene adipate terephthalate – PBAT; chitosan – CS; polyvinyl alcohol – PVA; cellulose diacetate – CD) was modified via plasma carbon coating to mainly change their physical surface properties, chemical composition, wettability and where applicable (if available as stable films) water barrier properties. As carbon coating for larger scales and geometrical changes (times, distances, and angles) the industrialized and commercially available FMC (flexible medical carbon), a DLC coating which is particularly applicable on soft substrates, was used.

- Objectives, challenges, deviations and duration extensions

Biopolymer material: In principle, there were no changes to the implementation of materials, equipment and objectives. Except for biopolymer PCL, which had to be excluded: a) no adequate thin films could be purchased on the market - only granulate and b) no corresponding knowledge and equipment to produce thin films is available. Therefore, it was replaced in the later work by available cellulose diacetate – CD films. In addition, studies on two further biopolymers CS and PVA from a new cooperation were included and results are published.

Synchrotron based analysis and corona:

Restrictions during the coronavirus period (coatings at NTT GmbH, canceled beamtimes at the synchrotron) and the failure of the necessary cooling circuit for the experimental setup in 2021 required a cost-neutral extensions of the project. Additional extensions were necessary due to the arrangement of new samples, a shortage of staff in 2022 and the fact that the synchrotron facility BESSYII unfortunately fell victim to a cyber-attack in June 2023 and went completely offline until the end of 2023 (important measures could not be carried out). We are extremely grateful to the DFG committee for the cost-neutral extensions to the project that were made possible for us, which enabled us to achieve our goals.

- Project-specific results and findings

For all used biopolymers (PLA, PHB, PBAT, CS, PVA, and CDA) the following industrial process was used to generate the DLC coatings: Biopolymer films were purchased in industrial quality and cut into respective pieces (mainly 10 x 10 cm or 10 x 5 cm) and carefully attached to self-built aluminum frames. Other probes than films were attached as smaller samples (via carbon tapes) to the holder in central positions. Holders were placed at 27.5 cm in front of the plasma source which corresponds to the established NTTF-GmbH coating process.^[12-14] Before each coating process, the samples were pre-treated with O₂-plasma for 10 min and subsequently the DLC layer was applied with C₂H₂, whereby the maximum temperature for the whole set-up does not exceed 40°C.^[5] According to the process illustrated in Fig. 1A, there are two main depositions: the direct (r-type, sample is facing the plasma source), and the indirect one (f-type, the sample is rotated 180° away), as described in Ref. [13].

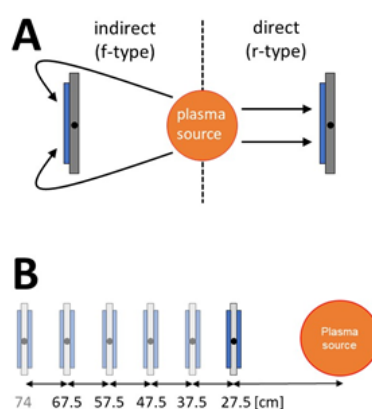


Fig. 1: Coating geometries: **A** standard process with the two extremes direct and indirect (based on Ref. [13]); **B** variations in distance in the direct configuration;

Fig. 1 **C**: coating geometries of the samples relative to the plasma source in 30° steps, all fixed at a 27.5 cm distance for the marked black pivot point.^[15]

Of interest are of course different distances and angle geometries to reach layer compositions in between of the two extremes. Therefore, the coating was arranged as depicted in Fig 1B and C. For B the distance to the source was successively increased from 27.5 to 67.5 cm in 10 cm steps, plus last one in the maximum distance of 74 cm, while maintaining the direct plasma configuration. For process C the samples were treated between the 0° (direct) and the 180° (indirect) configuration in 30° steps, whereby the pivot point (black dot marker point in Fig. 1C) was always positioned at the same distance of 27.5 cm from the source. All above mentioned polymer types were coated via the direct method A resp. in configuration C with 0° angle, to check their principal coatability.

Results for process B: In order to achieve a certain coating thickness, the coating rate was determined for PLA via process B. The deposition rate decreased with increasing distance

starting with 10 nm/min and dropping down to 1.6 nm/min at the maximum position of 74 cm. (each deposition time was 10 min). The wettability via contact angle (CA) was checked and showed a drop from the raw material, but only smaller deviations along the further process. Therefore, 27.5 cm as optimal point for sufficient layer thicknesses is used.

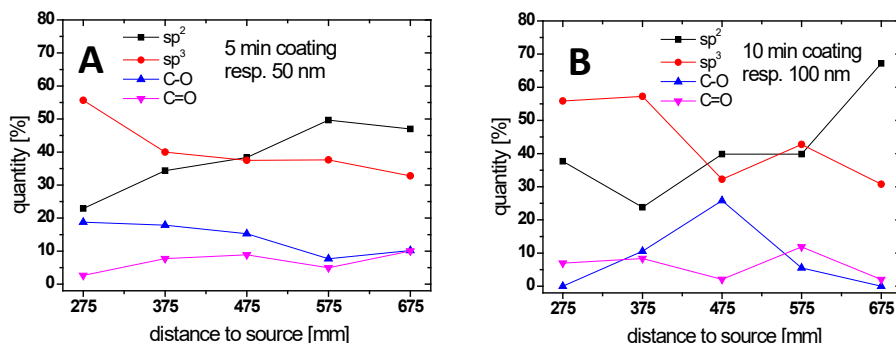


Fig. 2: Exemplary for PLA films: Components of the evaluated XPS C1s peaks plotted against the coating distance for 5 min in **A** and for 10 min in **B**.

Fig 2A and B shows the binding ratio change with increasing coating distance from sp^3 rich (red) near the source to a more sp^2 rich (black) from a distance of 47.5 cm for both. Thereafter, sp^2 remains the dominant bonding, with an exception for the 100 nm coating at 57.5 cm. The presence of O-bonds seems to decrease with increasing distance for the 50 nm coating. For the 100 nm a CO increase is recognizable at 47.5 cm (potentially due to ambient exposure during stress relief), but thereafter it decreases again. The observation is somewhat in line with former results for the f-type coating, increasing sp^2 content mostly on cost of the sp^3 content. In addition, the incident effect of the plasma in the direct configuration decreases with distance, as expected, an additional aspect for the distance of 27.5 cm.

General remarks for process C (Fig 1): The layer thickness at 30° and 60° was unfortunately not homogeneously distributed over the entire substrate surface due to a gradient caused by the coating geometry. The edge closer to the plasma source results in a bit thicker layer than the edge further away. The gradient increases with increasing angle, as the plasma hits the surface head-on. At 30° , a layer of 100 nm is applied in the middle, which deviates towards the edges $\sim 10\%$. At 60° , the coating thickness is also 100 nm in the center with a deviation of $\sim 20\%$ towards the edges. Therefore, for analytical purpose only probes from the center regions are considered. This is not the case for coating angles of 120 to 180° . Here, the sample films are exposed to indirect plasma, which is homogeneously distributed. As no significant change in the surface was observed at a treatment angle of 90° , this is not considered further below.

- **Results and published work for process A (Fig. 1A):**

Following process **A** (Fig. 1A) all biopolymers mentioned were subjected to this to test their basic coating capability and suitability for further angle-dependent configuration Fig. 1C. PLA and PHB were successfully included in the next phase of the project due to their performance

(see results for process **C** next section). In contrast, the delivered PBAT films were originally very soft and had a wavy appearance, which made them difficult to fix the entire probe completely flat in the holder. This resulted in cracks for already thin coatings as illustrated in Fig 3, where the SEM-morphology is correlated to the C1s proportions from XPS analysis. The break-up of the DLC layer at a thicknesses of 200/250 nm (red) and at 450–500 nm (green) can be explained by residual stress release of the coating and substrate combination. It can also be observed that these events are accompanied by a clear dominance change in the sp^2 to sp^3 ratios. Further details on PHB and PBAT films for this are published in the Refs. [16] and [17].

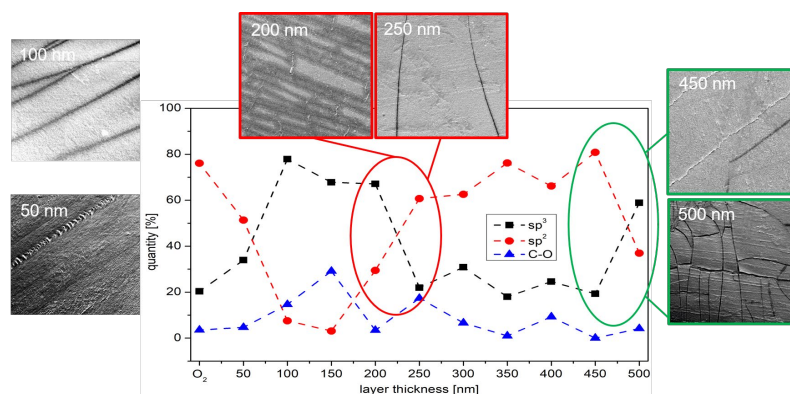
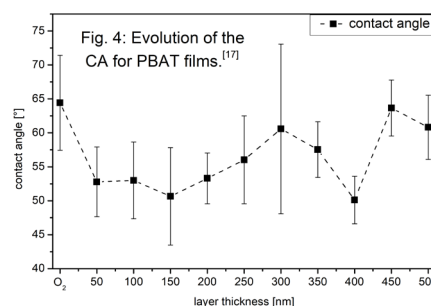


Fig. 3: For PBAT films the SEM morphology in relation to the changing C1s bonding states from XPS measures (based on Ref. [17]).

Summary on [16]: The amorphous hydrogenated carbon (a-C:H) layers are deposited on PHB using RF-PECVD. Layer thicknesses ranged from 0 to 500 nm by direct deposition (Fig. 1A). The study employed SEM, CA measurements, DRIFT spectroscopy, NEXAFS, and XPS to assess the morphology, wettability, and chemical structure of the coatings. The application of a-C:H coatings on PHB is possible and offers tunable surface properties, with layer thickness strongly influencing bonding hybridization. Results support the possibility to tailor biopolymer surfaces via controlled deposition, despite limitations at critical thicknesses. Therefore, a maximum of 100 nm for the depositions in process **C** is a good choice.

Summary on [17]: The deposition and characteristics of a-C:H coatings ranging from 0 to 500 nm on PBAT films using RF-PECVD are studied. The key objective is to assess how layer thickness affects the chemical structure and surface properties. The applied C coatings significantly modified the surface chemistry but with thickness-dependent instabilities. XPS confirmed dominant sp^3 bonds up to 200 nm, switching to sp^2 at 250–450 nm, and back to sp^3 at 500 nm (see Fig. 3). The polymer itself was excluded from further investigations in process **C** due to its original weakness and layer instability, which is exemplary shown in the variations of the CA with extremely high error margins in Fig. 4.



The stress release phenomena triggered the following studies, parts for PHB are published in [18] and for the development of the interlayer formation for PHB and PLA in [19]. The influence of residual stress in a-C:H layers here deposited on PHB and PLA films are studied by comparing two mechanical attachment conditions the coating: “fixed” (clamped on all sides) and “free” (clamped on one side only, see Fig 5A).

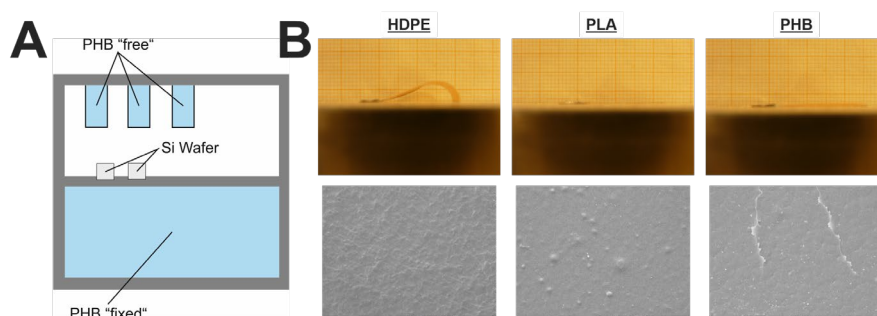


Fig 5: A Exemplary for PHB the samples holder set-up.^[18] The “free” PHB sized 1 x 2 cm at the top are free; the “fixed” sample is 5 x 10 cm and clamped fix on all four sides. **B:** SEM studies compared to curvature radius: HDPE shows strongest curvature but a smooth film; PLA is not visibly bended with film still smooth; PHB^[18] is slightly bended and film is clearly broken. This supports the distinct interlayer for HDPE^[13], a weaker interlayer for PHB as indicated in Ref. [5] and proven for PLA^[19], but not as pronounced, as stress destroys the coating.

Four layers (10, 50, 120, 170 nm) were applied on high-density polyethylene (HDPE), PHB and PLA. A comparison clearly revealed stress release phenomena for the biopolymers, but none for HDPE (Fig. 5B, partially unpublished results). By measuring the curvature radii prior to and upon coating, the stress produced in the layered composite was calculated via the Stoney equation. Results showed for PHB, that although the layer thickness increased, the stress in the layer decreased, due to the increasingly pronounced stress release phenomena.

Summary on [18]: Sample fixation during a-C:H deposition critically determines the layer integrity on PHB. Fixed samples support stable coatings with more sp²-dominated bonds at higher thicknesses reducing intrinsic stress. In contrast, free samples exhibit stress-induced failure and maintain a sp³ dominance. These findings are essential for industrial applications where coating stability not only on flexible biopolymers is required.

Summary on [19]: The influence of substrate chemistry on the formation of interlayers between a-C:H on PLA and PHB is investigated. Layers in the range of 0–50 nm were applied in 10 nm steps. AFM, XPS, NEXAFS, and IR spectroscopy are used to analyze and determine interlayer thickness. Interlayer formation during a-C:H coating could be proven and is strongly influenced by the substrate chemistry. Although PHB and PLA differ by only one C atom, the interlayer on PLA is twice as thick; 40 nm for PLA and 20 nm for PHB.

Further published contributions for process A: Direct a-C:H coating was also applied on nanoparticulate refined chitosan (CS, Ref. [20]) and microfiber reinforced polyvinyl alcohol (PVA, Ref. [21]) samples, as part of the cooperation with the University Mohammed IV Polytechnique

in Marocco. Both studies showed the basic coating capability with a-C:H (50 and 100 nm) and revealed already substrate-specific changes during the growth of the applied carbon layers.

- Results for process C (Fig. 1C):

Following process C (Fig. 1C), only the biopolymers PLA and PHB were subjected to this procedure due to their stable coating capability (chosen to the maximum of 100 nm resp. 10 min of direct coating duration at 27.5 cm) and intrinsic stability. Since each coating process is preceded by a 10 min treatment with O₂-plasma, which was originally adopted from the industrial process as such for cleaning, it is reasonable to check what effects this would have on the samples at different angles. Therefore, PLA and PHB pieces were arranged in the sample holders as following: each in the dimension of 5 x 10 cm (half holder dimension), one clamped tight and flat on the top half and the other one on the lower half (compare Fig. 5A), for identical conditions. Beside of the structural and compositional changes, determined by SEM, AFM and synchrotron analysis, it is worth to emphasize the findings for the wettability and permeability. As illustrated in Fig. 6A both materials became more hydrophilic after the O₂-plasma treatment.

Fig. 6: **A** CA of the angle-dependent O₂-plasma treatment for PLA and PHB (first value is the raw material). **B** WVTR values of the PLA and PHB films untreated (first value) and treated for 10 min with O₂-plasma with advancing angle geometries. The left y-axis presents the WVTR for PLA (black) and the right y-axis for the PHB (red, note different scaling).^[15]

The CA of PLA (black) reduced most sharply at 0° with a slight increase towards higher angles. For PHB, the CA decreases continuously until the 60° angle, increases slightly at towards 120°, indicating a decreasing sp³ content and fluctuates slightly thereafter. For the SFE the polar component of PLA peaked respectively at 0° and decreased thereafter with the angle processing, the disperse component mostly fluctuated. For PHB the polar component increased interestingly at higher angles (150°–180°), while the disperse component is as similar to PLA. The determined barrier properties resp. WVTR-values as shown in Fig. 6B delivered an 18% improvement for PLA at 120° (indicated in black). In contrast, PHB exhibits a clear increase in transmission rate for all angles, resulting in a 10% higher permeability.

Summary on [15]: This study shows how the applied angular variation in O₂-plasma treatments originally intended for cleaning already tailors surface properties of biopolymers and activates them for the carbon deposition. For PLA, indirect plasma improves the barrier performance. For PHB interestingly, oxidation even increases permeability, with structural integrity largely preserved, which is a very important information for the subsequent carbon coating process. Next, the impact of the angle-dependent a-C:H plasma on PLA by applying four different coating times (2.5, 5.0, 7.5, 10.0 min) is explored. The effect is studied by means of morphology, wettability, barrier properties, and chemical structure with more details in Ref. [22]. Fig. 7A presents AFM showing the morphology of the layers after 10 min at different angles. The DLC

application produces an opaque, (almost) homogeneous layer depending on the angle. The structural changes clearly indicate that the applied geometry has an influence. The roughness R increases with a maximum at 60° (R_a and R_q , see Table Fig. 7A). This also influences the CA (Fig. 7B), the surface energy (in Ref. [22]) and the resulting barrier properties (Fig. 7C).

Fig. 7: **A** AFM images of a-C:H coatings after 10 min angular plasma treatment. **B** Angle depended CA at 2.5, 5.0, 7.5 and 10.0 min treatment. The values are presented minus the respective O₂-pre-treated value (left gray bar presents untreated PLA with 78°). **C** Angle depended WVTR values at the respective treatment times minus the corresponding O₂ reference transmittance data from Ref. [15] (left grey bar presents the corresponding untreated PLA).^[22]

Summary on [22]: Altering the deposition angle and deposition time, the sp²/sp³ ratio in the applied a-C:H layers on PLA can be tuned in line with the surface properties. As a main result, optimal coating performance is achieved from 0° to 60° . The findings support the application of angle-dependent depositions as a control for an impactful strategy to modify the surface of (bio-)polymer materials. The work on PHB is yet unpublished, but submitted (see appendix a)

- Data handling

Raw data, results obtained and produced manuscripts resp. their metadata have been stored on a RAID network storage. The storage is localized only in the intranet, secured by a firewall and only visible and accessible to users who have been granted access by the PI. The PI is also the person responsible for the curation and later use of the data in regard of alternative data processing or use for follow-up projects. The research results have been and will continue to be made available to the scientific community in form of presentations (also included in specialized lectures in diverse study programs) and publications (as yet unpublished work).

- Bibliography

- [1] A.L. Andradý, M.A. Neal. *Philos. Trans. R. Soc., B* **2009**, 364, 1526 (1977–1984), DOI: [10.1098/rstb.2008.0304](https://doi.org/10.1098/rstb.2008.0304).
- [2] L. Sabbatini: Polymer surface characterization. De Gruyter graduate. DeGruyter, Berlin and Boston, **2014**.
- [3] J. Robertson. *Mater. Sci. Eng., R* **2002**, 37, (129–281), DOI: [10.1016/S0927-796X\(02\)00005-0](https://doi.org/10.1016/S0927-796X(02)00005-0).
- [4] J. Robertson. *Jpn. J. Appl. Phys.* **2011**, 50, 01AF01, DOI: [10.1143/JJAP.50.01AF01](https://doi.org/10.1143/JJAP.50.01AF01).
- [5] M. Rohrbeck et al. *Thin Solid Films* **2013**, 545 (558–563), DOI: [10.1016/j.tsf.2013.07.028](https://doi.org/10.1016/j.tsf.2013.07.028).
- [6] A. Grill. *IBM J. Res. & Dev.* **1999**, 43 (147–162), DOI: [10.1147/rd.431.0147](https://doi.org/10.1147/rd.431.0147).
- [7] R. Asakawa et al. *Surf. Coat. Technol.* **2011**, 206 (676–685), DOI: [10.1016/j.surf-coat.2011.02.064](https://doi.org/10.1016/j.surf-coat.2011.02.064).
- [8] R. Paul et al. *J. Phys. D: Appl. Phys.* **2008**, 41, 55309, DOI: [10.1088/0022-3727/41/5/055309](https://doi.org/10.1088/0022-3727/41/5/055309).
- [9] A. Grill. *Diam. Relat. Mater.* **2003**, 12 (166–170), DOI: [10.1016/S0925-9635\(03\)00018-9](https://doi.org/10.1016/S0925-9635(03)00018-9).
- [10] E. Mohagheghpour et al. *J. Mater. Res.* **2017**, 32, (1258–1266), DOI: [10.1557/jmr.2017.43](https://doi.org/10.1557/jmr.2017.43).
- [11] P. Couderc, Y. Catherine. *Thin Solid Films* **1987**, 146 (93–107), DOI: [10.1016/0040-6090\(87\)90343-9](https://doi.org/10.1016/0040-6090(87)90343-9).
- [12] A. Catena et al. *Carbon* **2016**, 96 (661–671), DOI: [10.1016/j.carbon.2015.09.101](https://doi.org/10.1016/j.carbon.2015.09.101).
- [13] C.B. Fischer et al. *Appl. Surf. Sci.* **2013**, 271 (381–389), DOI: [10.1016/j.apsusc.2013.01.210](https://doi.org/10.1016/j.apsusc.2013.01.210).
- [14] T. Schlebrowski, W. Rouabeh, S. Wehner, C.B. Fischer. *Thin Solid Films* **2019**, 691, 137617, DOI: [10.1016/j.tsf.2019.137617](https://doi.org/10.1016/j.tsf.2019.137617).

- **Published Project Results**

4.1 Category A – Articles in peer-reviewed journals, contributions to peer-reviewed conferences or to anthology volumes, and book publications

Publications (appendix 15-22)

- [15] L. Beucher, T. Schlebrowski, K. Rohe, S. Wehner, C.B. Fischer. *Surf. Interfaces* **2022**, 30, 101856. DOI: [10.1016/j.surfin.2022.101856](https://doi.org/10.1016/j.surfin.2022.101856).
- [16] T. Schlebrowski, L. Beucher, H. Bazzi, B. Hahn, S. Wehner, C.B. Fischer. *J. Carbon Res.* **2019**, 5 (3), 52 (1-12), DOI: [10.3390/c5030052](https://doi.org/10.3390/c5030052). - **Open Access**
- [17] T. Schlebrowski, H. Acharchi, B. Hahn, S. Wehner, C.B. Fischer. *Materials* **2020**, 13 (5), 1077, DOI: [10.3390/ma13051077](https://doi.org/10.3390/ma13051077). - **Open Access**
- [18] T. Schlebrowski, R. Ouali, B. Hahn, S. Wehner, C.B. Fischer. *Polymers* **2021**, 13 (2), 184, DOI: [10.3390/polym13020184](https://doi.org/10.3390/polym13020184). - **Open Access**
- [19] T. Schlebrowski, S. Wehner, C.B. Fischer. *Thin Solid Films* **2023**, 780, 139943 (1-9), DOI: [10.1016/j.tsf.2023.139943](https://doi.org/10.1016/j.tsf.2023.139943).
- [20] T. Schlebrowski, Z. Kassab, M. El Achaby, S. Wehner, C.B. Fischer. *J. Carbon Res.* **2020**, 6 (3), 51 (1-15), DOI: [10.3390/c6030051](https://doi.org/10.3390/c6030051). - **Open Access**
- [21] T. Schlebrowski, Z. Kassab, M. El Achaby, S. Wehner, C.B. Fischer, *Diamond Relat. Mater.* **2020**, 109, 108065 (1-8), DOI: [10.1016/j.diamond.2020.108065](https://doi.org/10.1016/j.diamond.2020.108065).
- [22] L. Beucher, T. Schlebrowski, M. Fritz, S. Wehner, C.B. Fischer. *Appl. Surf. Sci.* **2023**, 629, 157450 (1-10), DOI: [10.1016/j.apsusc.2023.157450](https://doi.org/10.1016/j.apsusc.2023.157450)

4.2 Category B – Any other form of published results

none

4.3 Patents (applied for and granted)

none